









BRIEF COMMUNICATION

# Unique Transcriptome Signature Distinguishes Patients With Heart Failure With Myopathy

Talia Caspi , MBChB\*; Sam Straw , MBChB\*; Chew Cheng , PhD\*; Jack O Garnham, PhD; Jason L. Scragg, PhD; Jessica Smith, PhD; Aaron O. Koshy, MBChB; Eylem Levelt, PhD; Piruthivi Sukumar , MD; John Gierula, PhD; David J. Beech, PhD; Mark T. Kearney , MD; Richard M. Cubbon , PhD; Stephen B. Wheatcroft, PhD; Klaus K. Witte , MD; Lee D. Roberts, PhD; T. Scott Bowen , PhD

**BACKGROUND:** People with chronic heart failure (CHF) experience severe skeletal muscle dysfunction, characterized by mitochondrial abnormalities, which exacerbates the primary symptom of exercise intolerance. However, the molecular triggers and characteristics underlying mitochondrial abnormalities caused by CHF remain poorly understood.

**METHODS AND RESULTS:** We recruited 28 patients with CHF caused by reduced ejection fraction and 9 controls. We simultaneously biopsied skeletal muscle from the pectoralis major in the upper limb and from the vastus lateralis in the lower limb. We phenotyped mitochondrial function in permeabilized myofibers from both sites and followed this by complete RNA sequencing to identify novel molecular abnormalities in CHF skeletal muscle. Patients with CHF presented with upper and lower limb skeletal muscle impairments to mitochondrial function that were of a similar deficit and indicative of a myopathy. Mitochondrial abnormalities were strongly correlated to symptoms. Further RNA sequencing revealed a unique transcriptome signature in CHF skeletal muscle characterized by a novel triad of differentially expressed genes related to deficits in energy metabolism including adenosine monophosphate deaminase 3, pyridine nucleotide-disulphide oxidoreductase domain 2, and lactate dehydrogenase C.

**CONCLUSIONS:** Our data suggest an upper and lower limb metabolic myopathy that is characterized by a unique transcriptome signature in skeletal muscle of humans with CHF.

**Key Words:** chronic heart failure ■ metabolism ■ mitochondria ■ skeletal muscle

People with chronic heart failure (CHF) caused by reduced left ventricular ejection fraction (ie, heart failure with reduced ejection fraction) develop significant skeletal muscle abnormalities underpinned by impaired mitochondrial energy metabolism, which more closely correlate to symptoms than to the degree of cardiac dysfunction.<sup>1</sup> Improved skeletal muscle mitochondrial function in CHF is associated with alleviation of symptoms and improved quality of life, and is considered a worthy therapeutic target.<sup>2</sup> However, controversy remains as to whether

muscle mitochondrial abnormalities in CHF are central to the disease process or occur secondary to detraining.<sup>3</sup> Most studies in patients with CHF have used thigh biopsies to investigate mitochondrial dysfunction,<sup>1</sup> while few studies have used alternative sample sites that are unlikely impacted by detraining. Yet, various upper limb muscles (eg, pectoralis major and diaphragm) in patients with CHF exhibit histological perturbations similar to (or even greater than) the lower limbs (eg, vastus lateralis).<sup>1</sup> The pectoralis major also demonstrates mitochondrial dysfunction<sup>4</sup>

Correspondence to: T. Scott Bowen, PhD, School of Biomedical Sciences, Faculty of Biological Sciences, University of Leeds, Leeds LS2 9JT, United Kingdom. E-mail: t.s.bowen@leeds.ac.uk

Supplementary Materials for this article are available at <https://www.ahajournals.org/doi/suppl/10.1161/JAHA.120.017091>

\*Dr Caspi, Dr Straw, and Dr Cheng contributed equally to this work.

For Sources of Funding and Disclosures, see page 8.

© 2020 The Authors. Published on behalf of the American Heart Association, Inc., by Wiley. This is an open access article under the terms of the Creative Commons Attribution License, which permits use, distribution and reproduction in any medium, provided the original work is properly cited.

JAHA is available at: [www.ahajournals.org/journal/jaha](http://www.ahajournals.org/journal/jaha)

alongside muscle atrophy that independently predicts mortality in patients with CHF.<sup>2</sup> This evidence provides support for a myopathy in patients with CHF independent of detraining.

The mechanisms underpinning mitochondrial dysfunction in CHF remain poorly defined. Putative mechanisms specific to the disease include impaired energy homeostasis via dysregulation in high energy phosphates (eg, ATP, ADP, and AMP), activation of atrophic signaling networks involved in protein degradation, elevated inflammatory cytokines and reactive O<sub>2</sub> species that disrupt cellular homeostasis, and abnormal microvascular homeostasis.<sup>1</sup> Yet, many of these hypotheses have been investigated in animal models rather than human tissue. Whole transcriptome RNA sequencing (RNA-seq) has been applied in people with diabetes mellitus,<sup>5</sup> critical illness,<sup>6</sup> peripheral arterial disease,<sup>7</sup> disuse,<sup>8</sup> and aging<sup>9</sup> to reveal novel molecular mechanisms of skeletal muscle abnormalities. However, to our knowledge, the molecular signature of skeletal muscle in patients with CHF has yet to be investigated.

Here, we recruited a total of 28 patients with CHF and 9 controls. We simultaneously biopsied skeletal muscle from the pectoralis major (PM) in the upper limb and from the vastus lateralis (VL) in the lower limb. Mitochondrial function was phenotyped in myofibers from both sites using high-resolution respirometry to determine whether upper and lower limb impairments were present and their association with symptoms. We then applied RNA-seq to identify underlying molecular abnormalities of muscle dysfunction in patients with CHF. Overall, we found that patients with CHF present with a similar degree of mitochondrial dysfunction in both the PM and VL, indicative of a myopathy. RNA-seq analysis identified a triad of differentially expressed genes related to impaired mitochondrial energy metabolism. We believe our data reveal, for the first time, a unique transcriptome signature in skeletal muscle of humans with CHF.

## METHODS

The data that support the findings of this study are available from the corresponding author upon reasonable request. Clinical characteristics and medications for all patients are presented in Tables S1 and S2, respectively. Patients were allocated to control (n=9) or CHF (n=28) groups. Controls had no clinical evidence of CHF: left ventricular ejection fraction  $\geq 50\%$  and no previous diagnosis of left ventricular systolic dysfunction. Patients with CHF had stable symptoms of CHF (>3 months on medical therapy) and a left ventricular ejection fraction <50% as confirmed by

transthoracic echocardiography (following current European Society of Cardiology guidelines). All participants were indicated for device therapy with either a permanent pacemaker, implantable cardioverter-defibrillator, or cardiac resynchronization therapy device according to current indications. Patients with CHF performed a peak symptom-limited exercise test to volitional exhaustion on a cycle ergometer for determination of peak pulmonary O<sub>2</sub> uptake (VO<sub>2peak</sub>). Exclusion criteria included inability to provide informed consent because of cognitive dysfunction or the presence of previous diagnoses with other potentially confounding comorbidities, such as chronic obstructive pulmonary disease or cancer. All patients provided written informed consent and all procedures were conducted in accordance with the Declaration of Helsinki after receiving local institute ethical approval (11/YH/0291).

## Muscle Biopsy, Mitochondrial Respiration, and RNA-Seq

Muscle samples were taken from 2 sites in participants: the upper limb (PM) and lower limb (VL). The PM sample was obtained during routine device implantation procedures, while on the same day the VL sample was from the right thigh. One piece of fresh muscle sample was used for the assessment of mitochondrial respiration,<sup>4</sup> while another small portion was rapidly frozen in a subset of patients (controls=3, CHF=6) for subsequent RNA-seq analysis.<sup>10</sup> See Data S1 for expanded details.

## Statistical Analysis

Assumption of homogeneity of variance was confirmed using Levene test, while Shapiro-Wilk and Kolmogorov-Smirnov normality tests confirmed normal (Gaussian) distribution. Unpaired Student *t* test was used to compare between-group differences, while paired Student *t* test was used for within-group comparisons for continuous data and chi-square test for categorical data. Further, ANCOVA was performed to adjust for the variables of age and sex. Pearson correlation coefficient (*r*) was performed to assess the association between mitochondrial respiration at different muscle sites and VO<sub>2peak</sub>. Continuous data are expressed as mean $\pm$ SEM and categorical data as number (percentage). Statistical significance was accepted as *P*<0.05.

## RESULTS

### Mitochondrial Myopathy in Patients With CHF

We first aimed to confirm the presence of skeletal muscle mitochondrial dysfunction in patients with CHF

in both upper and lower limb muscle sites. Based on published data, we hypothesized that mitochondrial dysfunction would occur to a greater degree in the lower compared with the upper limbs. We analyzed mitochondrial  $O_2$  consumption in permeabilized fibers of PM and VL from patients with CHF using high-resolution respirometry. Mitochondrial  $O_2$  flux was, on average, lower by 15% to 20% in patients with CHF among respiratory states (Figure 1A and 1B). ADP-stimulated mitochondrial complex I respiration was lower in both PM ( $P=0.028$ ) and VL ( $P=0.015$ ) by 25% and 28%, respectively (Figure 1A and 1B). Convergent complex I and II respiration ( $P=0.047$ ) and complex II respiration ( $P=0.037$ ) were also significantly lower in the PM of patients with CHF compared with controls by  $\approx 20\%$  (Figure 1A). However, after adjusting for confounding variables (specifically age and sex) between the 2 groups, differences in mitochondrial respiration were not detected ( $P>0.05$ ). Mitochondrial respiration is determined by both organelle quantity and quality. A lower mitochondrial content is most often reported in patients with CHF.<sup>3,11</sup> We therefore assessed intrinsic mitochondrial respiration after normalization to complex IV activity (a proxy for mitochondrial mass).<sup>4</sup> Here, we observed fewer differences between patients and controls (Figure 1C and 1D), with only VL showing an 18% lower complex I respiration versus controls ( $P=0.048$ , Figure 1D).

### Whole-Body Mitochondrial Impairments Correlate to Symptoms

Having identified that both upper and lower muscles of patients with CHF experience similar reductions in mitochondrial respiration, we further characterized their clinical importance. We correlated mitochondrial deficits in PM and VL to the gold-standard measure of whole-body exercise intolerance: peak pulmonary  $O_2$  uptake ( $VO_{2peak}$ ). We focused on complex I and complex IV respiration, given our earlier findings. Complex I respiration was well correlated with  $VO_{2peak}$  in PM but less so in VL (Figure 1E and 1F), while complex IV respiration correlated well with measures in PM but not VL (Figure 1G and 1H).

### Lower Limbs Demonstrate Greater Oxidative Capacity

The PM and VL demonstrated distinct phenotypes in correlations between mitochondrial mass and exercise intolerance. Therefore, we compared mitochondrial respiration between PM and VL muscle sites in patients with CHF for mechanistic insight. Compared with PM, patients with CHF demonstrated greater mitochondrial  $O_2$  flux in VL across respiratory states. Both complex I and complex II respiration were  $\approx 30\%$

higher in VL versus PM ( $P<0.001$ ). Mitochondrial content, as assessed by complex IV respiration, was also higher in VL versus PM by  $\approx 40\%$  (Figure 2A). We therefore normalized PM and VL respiration to mitochondrial content to assess intrinsic respiration. PM had higher intrinsic mitochondrial respiration at leak ( $P=0.01$ ) and complex I ( $P=0.02$ ) compared with VL (Figure 2B); however, no differences between the respiratory control ratio (RCR) was detected ( $5.0\pm 0.6$  versus  $5.4\pm 0.4$ ,  $P>0.05$ ). Furthermore, complex I respiration was correlated between upper and lower limb muscles ( $r=0.51$ ,  $P=0.02$ ; Figure 2C). This was not observed for complex IV respiration ( $r=0.22$ ,  $P=0.32$ ; Figure 2D).

### RNA-Seq Analysis in Human Heart Failure Skeletal Muscle

We have demonstrated that mitochondrial dysfunction induced by CHF occurs in both the upper and lower limbs that closely correlates to symptom severity. Next, we used high-throughput RNA-seq to interrogate the molecular alterations accompanying skeletal muscle impairments in CHF (Figure 3A). To our knowledge, our study is the first to perform whole-transcriptome sequencing in skeletal muscle in humans with CHF. RNA-seq was performed on PM biopsy from 9 participants (3 controls and 6 CHF, Table S3), which generated  $\approx 16$  million 75 bp single-end reads for each individual (Table S4). Only uniquely mapped reads were retained for downstream differential expression analysis. Overall,  $\approx 92\%$  of the reads mapped uniquely to the human reference genome (GRCh38). RNA integrity number scores were consistently high for all samples (RNA integrity number  $>7.5$ ). The read counts were normalized using median of ratios as implemented in *DESeq2*. The normalized gene expression was expressed as read counts for all 18 426 genes (Table S5). To determine whether expression profiles among the 9 patients could discriminate them based on the disease status, the data set was analyzed using partial least squares discriminant analysis. Partial least squares discriminant analysis plot distinguished 2 groups of individuals: controls and patients with CHF (Figure 3B). The first component accounted for 48%, and the second component accounted for 21% of the variance in the partial least squares discriminant analysis model. Interestingly, our transcriptome analysis also appeared to identify 2 distinct clusters of patients with CHF (Figure 3B): cluster 1 ( $n=3$ ; patients 1, 3, and 4) and cluster 2 ( $n=3$ ; patients 2, 5, and 6). When we further analyzed demographic and clinical characteristics of these 2 clusters (Table S6) we found only left ventricular systolic function to be different between the 2 groups, with a lower value in cluster 2

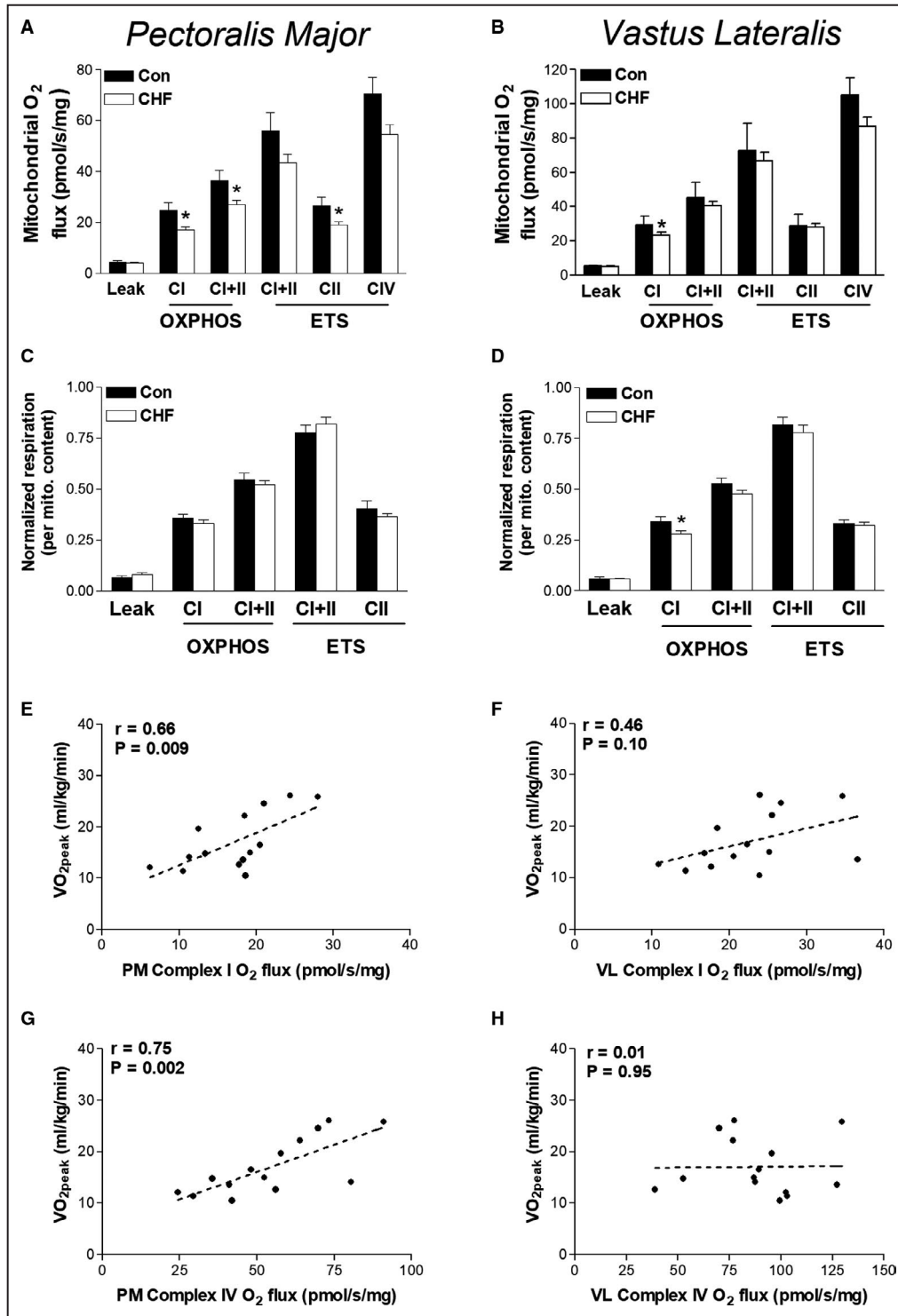


**Figure 1. Skeletal muscle mitochondrial respiration is impaired in patients with heart failure and correlated to exercise intolerance.**

Mitochondrial O<sub>2</sub> flux measured in myofibers biopsied from pectoralis major (PM) and vastus lateralis (VL) of patients with chronic heart failure (CHF) (n=22) and controls (n=6). Mitochondrial respiration in the PM and VL is presented between groups in both absolute units (A and B) and normalized to mitochondrial content (C and D). Correlations between exercise intolerance (ie, VO<sub>2peak</sub>) and complex I respiration (E and F) and mitochondrial content (ie, complex IV) in CHF (G and H). Leak (L<sub>i</sub>), complex I (P<sub>i</sub>), complex I and II (P<sub>i+II</sub> and E<sub>i+II</sub>), complex II (E<sub>ii</sub>) and complex IV (C<sub>iv</sub>) measured under oxidative phosphorylation (OXPHOS; P), and electron transport system (ETS; E) supported respiration. \*P<0.05 between-group comparisons. Correlation coefficient (r). Data are mean±SEM.

Downloaded from <http://ahajournals.org> by on September 11, 2020

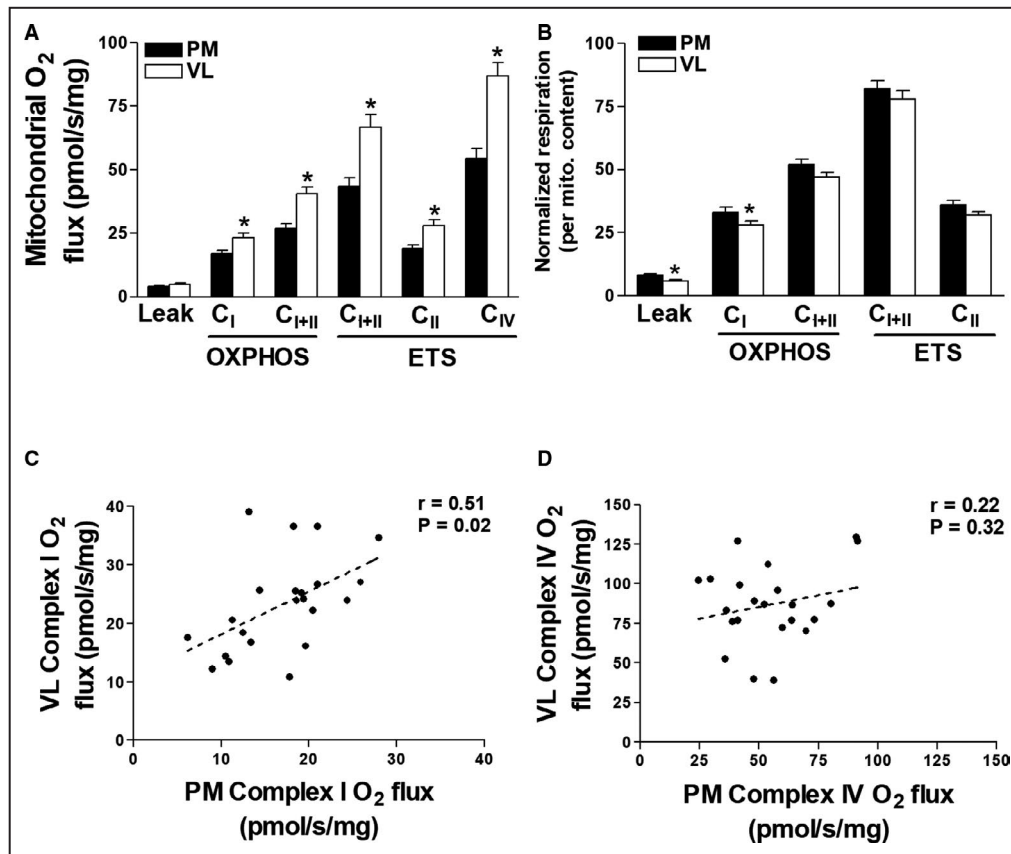


**Figure 2.** Mitochondrial respiration varies between upper and lower limb skeletal muscle in patients with heart failure.

Pectoralis major (PM) and vastus lateralis (VL) mitochondrial respiration measured in myofibers of patients with chronic heart failure (CHF) (A) and corrected for mitochondrial content (B). Correlations between VL and PM complex I function (C) and complex IV function (mitochondrial content) (D). Leak (L<sub>i</sub>), complex I (P<sub>i</sub>), complex I and II (P<sub>i+ii</sub> and E<sub>i+ii</sub>), complex II (E<sub>ii</sub>) and complex IV (C<sub>iv</sub>) measured under oxidative phosphorylation (OXPHOS; P) and electron transport system (ETS; E) supported respiration. \**P*<0.05. Correlation coefficient (*r*). Data are mean±SEM.

versus cluster 1 (14%±1% versus 38%±5%, *P*<0.01; Table S6). Taken together, these data may indicate that the degree of left ventricular systolic dysfunction is a potential determinant of the skeletal muscle transcriptome in patients with CHF.

### Distinct Transcriptome Signature in Skeletal Muscle of CHF

From a total of 18 426 genes identified, 3 genes related to energy metabolism were differentially expressed genes between control and CHF at a fold change >1.5 and false discovery rate threshold <0.05 (Figure 3C). Two genes were upregulated in CHF: AMP deaminase 3 (AMPD3) ( $\log_2$ -fold change=1.62, false discovery rate=0.0023) and pyridine nucleotide-disulphide oxidoreductase domain 2 (PYROXD2) ( $\log_2$ -fold change=1.33, false discovery rate=0.0077), while lactate dehydrogenase C ( $\log_2$ -fold change=-5.52, false discovery rate=0.0002) was downregulated (Figure 3C). Hierarchical clustering illustrated on the

heat map using the 3 differentially expressed genes clearly show 2 distinct branches. In patients with CHF we found that lactate dehydrogenase C was consistently downregulated among the 6 patients, while AMPD3 and PYROXD2 were upregulated (Figure 3D). Overall, whole-transcriptome sequencing revealed a novel triad of metabolic genes that are dysregulated in skeletal muscle from patients with CHF.

### DISCUSSION

This is the first study to demonstrate that skeletal muscle from patients with CHF is characterized by a unique transcriptome signature that underpins an upper and lower limb metabolic myopathy closely linked to worse symptoms. We identified a triad of genes dysregulated in CHF that are involved in ATP homeostasis. These findings have important implications for our understanding of the link between muscle abnormalities and symptoms in patients with CHF.



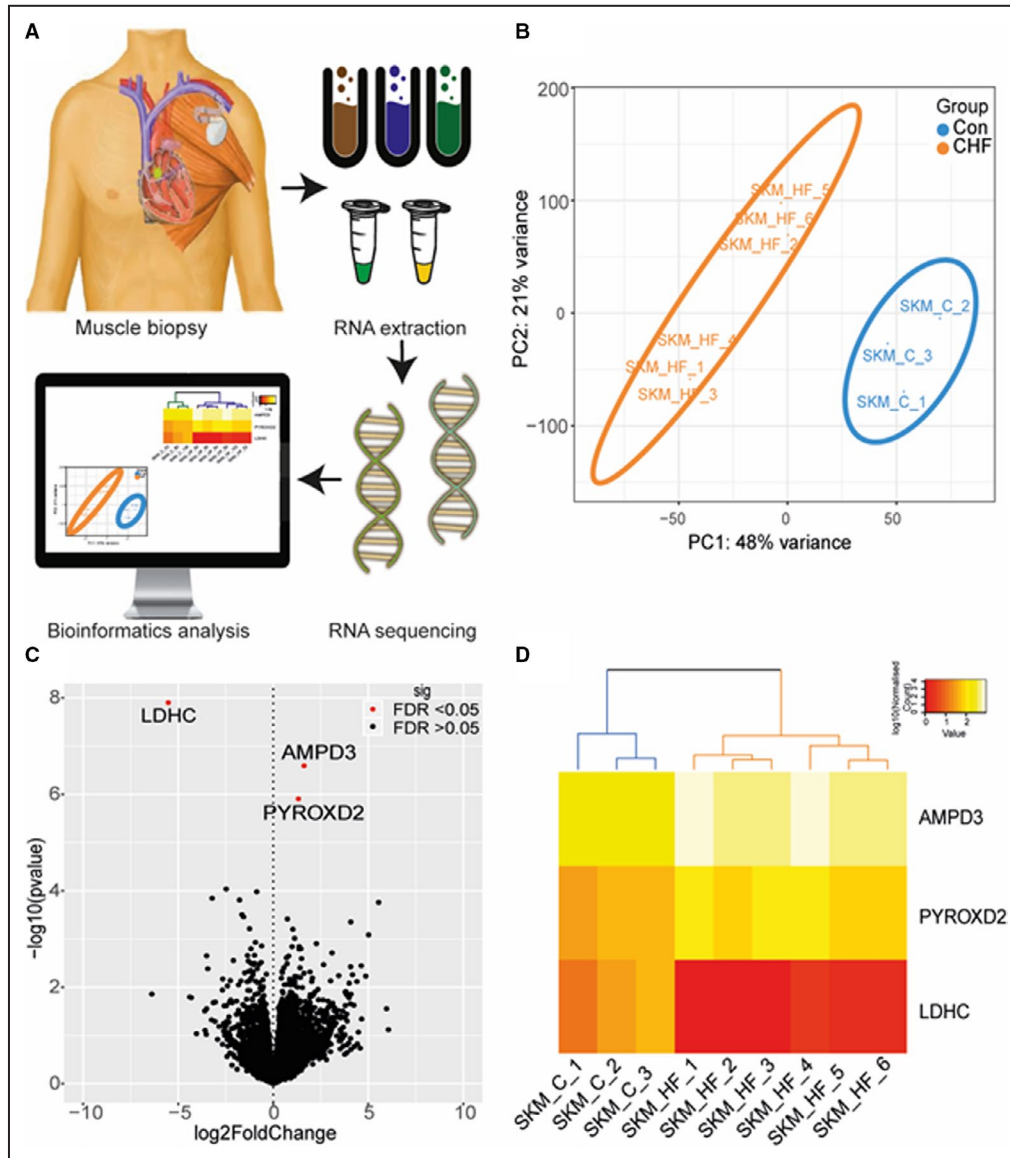


**Figure 3. Patients with heart failure are characterized by a distinct skeletal muscle transcriptome signature.**

RNA-sequencing analysis workflow (A), where 9 pectoralis major (PM) human biopsies were obtained (n=3 controls; n=6 chronic heart failure [CHF]) and RNA samples proceeded with library preparation and RNA sequencing. Bioinformatics processing was performed on the raw reads and identified the significantly regulated genes in CHF. Partial least squares discriminant analysis (PLS-DA) plot of expression profiles for 18 426 genes among the 9 patients, CHF (orange) controls (blue) (B). Volcano plot showing the 3 significantly regulated genes (red dots), including AMP deaminase 3 (AMPD3) and pyridine nucleotide-disulphide oxidoreductase domain 2 (PYROXD2) upregulated in CHF and lactate dehydrogenase C (LDHC) downregulated (C). Heat map of differentially expressed genes (DEGs) in CHF and control samples (D). DEGs in the heat map were clustered based on a hierarchical algorithm implemented in “pheatmap.” Heat map was generated with  $\log_{10}$ -normalized reads derived from *DESeq2*. Color scale represents  $\log_{10}$ -transformed normalized reads.

### Is There a CHF-Associated Myopathy?

Our data highlight that both PM and VL in patients with CHF show a similar degree of loss in mitochondrial respiratory function (Figure 1A and 1B). This upper and lower limb dysfunction appears primarily driven by a decrease in mitochondrial volume and

dysfunction of complex I respiration, which is likely a major contributor exacerbating symptoms of fatigue in many patients. We speculate that this could reflect a mitochondrial myopathy that is independent of disuse, which may exacerbate symptoms of exercise limitation (Figure 1E through 1H). Our findings

further revealed that while mitochondrial capacity is higher per muscle mass in the leg,  $O_2$  flux normalized per mitochondrial mass (ie, intrinsic function) is higher in the chest muscle (Figure 2A and 2B). Thus, it seems that the VL has higher mitochondrial mass compared with upper limb muscles, which is likely a consequence of higher metabolic demands during daily activities. This may be important because, unlike the VL, the PM did not demonstrate reductions in intrinsic mitochondrial function versus healthy controls. The close association between  $O_2$  flux measurements taken from chest and leg muscle further provides validation for the PM being an alternative site for investigating muscle dysfunction in patients with CHF, which aligns with recent data showing that PM muscle volume independently predicts mortality.<sup>2</sup>

### Is Lactate Dehydrogenase C Limiting Anaerobic Metabolism?

Patients with CHF have an increased reliance on anaerobic metabolism for a given exercise work load compared with matched controls,<sup>12</sup> which is caused by significant limitations to mitochondrial oxidative metabolism (Figure 1). Our RNA-seq analysis showed that the glycolytic enzyme lactate dehydrogenase C was severely downregulated by 46-fold in patients with CHF versus controls (Figure 3C and 3D), which is consistent with earlier work<sup>3,12</sup> and indicates disruptions to  $NAD^+$ / $NADH$  homeostasis in CHF skeletal muscle. Overall, these data implicate a specific impairment at the transcriptional level of the lactate dehydrogenase enzyme and identify components of both oxidative and glycolytic metabolic machinery to be perturbed in CHF.

### Is AMPD3 a Mediator of Impaired Metabolism and Fiber Atrophy?

The AMPD3 gene showed the highest upregulation in CHF by 3-fold (Figure 3C and 3D), which indicates a shift toward a greater reliance on the AMP deaminase reaction in skeletal muscle of patients with CHF. AMPD3 catalyzes the first and rate-limiting step of the purine nucleotide cycle, highlighting its role as a key enzyme muscle energetics and amino acid catabolism. Under metabolic stress, AMP levels increase as ADP is converted to ATP and AMP via the adenylate kinase reaction, which maintains a high ATP/ADP ratio. AMP is then irreversibly deaminated by AMP deaminase to inosine monophosphate and ammonia. In vivo evidence confirms intramuscular concentration of ADP are higher and Phosphocreatine (PCr) and pH are lower for given work rates in patients with CHF,<sup>12,13</sup> which could explain our transcriptome findings that AMPD3 expression is increased to compensate under metabolic stress where ATP is low

(Figures 1 through 3).<sup>12,13</sup> AMP activates glycolytic metabolism and this mechanism is likely impaired given the capacity of glycolytic enzymes is lower in muscle from patients with CHF.<sup>3,12</sup> Increased reliance on AMP deaminase would increase inosine monophosphate and ammonia formation while lowering the total adenine nucleotide pool thereby exacerbating muscle fatigue. Elevated levels of inosine monophosphate are converted back to AMP by combining with the amino acid aspartate via the purine nucleotide cycle. Increased expression of AMPD3 in skeletal muscle of patients with CHF may reflect a fuel shift toward increased catabolism of amino acids and thus provide a novel mechanism linking metabolic dysregulation and muscle wasting in patients with CHF given AMPD3 is upregulated in various atrophic conditions in animal models such as disuse, starvation, cancer, and denervation.<sup>14</sup> Here, we translate this to humans with CHF.

### Does PYROXD2 Link to Mitochondrial Dysfunction and Myopathy?

PYROXD2 was upregulated by 2.5-fold in patients with CHF (Figure 3C and 3D). The physiological role of PYROXD2, particularly in skeletal muscle, remains largely unclear but recent data show that genetic variants in its family member PYROXD1 induces early-onset myopathy and limb girdle muscular dystrophy characterized by abnormal myofibrils, nuclei, and mitochondria.<sup>15</sup> PYROXD2 is part of a pyridine nucleotide-disulfide oxidoreductase domain-containing protein family that is involved in redox and energy balance. Pyridine nucleotidedisulphide reductases are flavoproteins (FAD binding) that catalyze the pyridine nucleotide ( $NAD^+$ / $NADH$ )-dependent reduction of cysteine residues in their substrates,<sup>15</sup> implicating a role for impaired  $NAD^+$ / $NADH$  homeostasis. PYROXD2 (also known as YueF) can also induce the expression of the transcription factor p53,<sup>16</sup> with the latter known to promote fiber atrophy in various conditions including limb immobilization and cancer cachexia.<sup>17</sup> Overall, these studies identify PYROXD2 as a potential regulator of muscle homeostasis in patients with CHF by controlling metabolic homeostasis, mitochondrial function, and fiber atrophy via a redox-dependent pathway.

### Study Limitations

Our analyses were performed in a relatively small sample size, mostly men and patients with a reduced ejection fraction, so should be viewed with caution when generalizing to the larger population of patients with CHF. In addition, our in situ mitochondrial respiration measurements may not reflect the in vivo muscle environment in patients, given some of the

experimental settings such as O<sub>2</sub> and substrate (eg, ADP) concentrations where unphysiological (as detailed elsewhere<sup>18</sup>), which may limit translation. We have also inferred that mitochondrial impairments in skeletal muscle are likely contributing to symptoms of exercise intolerance to a greater degree than those related to cardiac dysfunction, as based on our correlative data. This suggestion is supported by clear data showing that exercise intolerance (ie, VO<sub>2peak</sub>) in patients with CHF poorly correlates with measures of cardiac dysfunction, while in contrast skeletal muscle impairments are closely associated.<sup>19</sup> We also acknowledge that some variance in our results may be explained, at least in part, by other confounding factors such as sex, age, and levels of physical activity.<sup>4,20</sup> As such, future studies should carefully control for potential confounding factors that may have impacted our current results.

## CONCLUSIONS

We believe this is the first study to demonstrate that patients with CHF are characterized by a unique transcriptome signature in skeletal muscle that is underpinned by a metabolic myopathy in both the upper and lower limbs, which closely associated with worse symptoms. These findings have important implications for our understanding of the skeletal muscle pathology and its relation to symptoms in patients with CHF.

## ARTICLE INFORMATION

Received April 15, 2020; accepted July 29, 2020.

### Affiliations

From the Leeds Institute of Cardiovascular and Metabolic Medicine (T.C., S.S., C.C., J.O.G., J.L.S., J.S., A.O.K., E.L., P.S., J.G., D.J.B., M.T.K., R.M.C., S.B.W., K.K.W., L.D.R.) and School of Biomedical Sciences, Faculty of Biological Sciences, University of Leeds, United Kingdom (T.S.B.).

### Acknowledgments

We thank Dr Richard Ferguson, Loughborough University, for expertise on the leg biopsy technique and the High-Performance Computing facilities at University of Leeds for bioinformatics analyses.

### Sources of Funding

This work was supported by Leeds Cardiovascular Endowment Fund. Straw by British Heart Foundation Clinical Fellowship. Roberts by Diabetes UK RD Lawrence Fellowship (16/0005382). Cubbon by British Heart Foundation Intermediate Research Fellow. Kearney British Heart Foundation Chair of Cardiology. Witte by National Institute for Health Research (NIHR) Clinician Scientist Award. Bowen by Medical Research Council UK (MR/S025472/1) and Heart Research UK (TRP 16/19).

### Disclosures

None.

### Supplementary Materials

Data S1

Tables S1–S6

## REFERENCES

1. Kennel PJ, Mancini DM, Schulze PC. Skeletal muscle changes in chronic cardiac disease and failure. *Compr Physiol*. 2015;5:1947–1969.
2. Kumar A, Ansari BA, Kim J, Suri A, Gaddam S, Yenigalla S, Vanjarapu JM, Selvaraj S, Tamvada D, Lee J, et al. Axial muscle size as a strong predictor of death in subjects with and without heart failure. *J Am Heart Assoc*. 2019;8:e010554. DOI: 10.1161/JAHA.118.010554
3. Mettauer B, Zoll J, Sanchez H, Lampert E, Ribera F, Veksler V, Bigard X, Mateo P, Epailly E, Lonsdorfer J. Oxidative capacity of skeletal muscle in heart failure patients versus sedentary or active control subjects. *J Am Coll Cardiol*. 2001;38:947–954.
4. Garnham JO, Roberts LD, Caspi T, Al-Owais MM, Bullock M, Swoboda PP, Koshy A, Gierula J, Paton MF, Cubbon RM, et al. Divergent skeletal muscle mitochondrial phenotype between male and female patients with chronic heart failure. *J Cachexia Sarcopenia Muscle*. 2019;11:394–404.
5. Scott LJ, Erdos MR, Huyghe JR, Welch RP, Beck AT, Wolford BN, Chines PS, Didion JP, Narisu N, Stringham HM, et al. The genetic regulatory signature of type 2 diabetes in human skeletal muscle. *Nat Commun*. 2016;7:11764.
6. Llano-Diez M, Fury W, Okamoto H, Bai Y, Gromada J, Larsson L. RNA-sequencing reveals altered skeletal muscle contraction, E3 ligases, autophagy, apoptosis, and chaperone expression in patients with critical illness myopathy. *Skelet Muscle*. 2019;9:9.
7. Ryan TE, Yamaguchi DJ, Schmidt CA, Zeczycki TN, Shaikh SR, Brophy P, Green TD, Tarpey MD, Karnekar R, Goldberg EJ, et al. Extensive skeletal muscle cell mitochondriopathy distinguishes critical limb ischemia patients from claudicants. *JCI Insight*. 2018;3:e123235.
8. Mahmassani ZS, Reidy PT, McKenzie AI, Stubben C, Howard MT, Drummond MJ. Disuse-induced insulin resistance susceptibility coincides with a dysregulated skeletal muscle metabolic transcriptome. *J Appl Physiol (1985)*. 2019;126:1419–1429.
9. Robinson MM, Dasari S, Konopka AR, Johnson ML, Manjunatha S, Esponda RR, Carter RE, Lanza IR, Nair KS. Enhanced protein translation underlies improved metabolic and physical adaptations to different exercise training modes in young and old humans. *Cell Metab*. 2017;25:581–592.
10. Conesa A, Madrigal P, Tarazona S, Gomez-Cabrero D, Cervera A, McPherson A, Szczesniak MW, Gaffney DJ, Elo LL, Zhang X, et al. A survey of best practices for RNA-seq data analysis. *Genome Biol*. 2016;17:13.
11. Garnier A, Fortin D, Zoll J, N'Guessan B, Mettauer B, Lampert E, Veksler V, Ventura-Clapier R. Coordinated changes in mitochondrial function and biogenesis in healthy and diseased human skeletal muscle. *FASEB J*. 2005;19:43–52.
12. Mancini DM, Coyle E, Coggan A, Beltz J, Ferraro N, Montain S, Wilson JR. Contribution of intrinsic skeletal muscle changes to <sup>31</sup>P NMR skeletal muscle metabolic abnormalities in patients with chronic heart failure. *Circulation*. 1989;80:1338–1346.
13. Massie B, Conway M, Yonge R, Frostick S, Ledingham J, Sleight P, Radda G, Rajagopalan B. Skeletal muscle metabolism in patients with congestive heart failure: relation to clinical severity and blood flow. *Circulation*. 1987;76:1009–1019.
14. Miller SG, Hafen PS, Braut JJ. Increased adenine nucleotide degradation in skeletal muscle atrophy. *Int J Mol Sci*. 2019;21:8.
15. O'Grady GL, Best HA, Sztal TE. Variants in the oxidoreductase pyroxd1 cause early-onset myopathy with internalized nuclei and myofibrillar disorganization. *Am J Hum Genet*. 2016;99:1086–1105.
16. Huang J, Kailang W, Zhang J, Si W, Zhu Y, Wu J. Putative tumor suppressor YueF affects the functions of hepatitis B virus X protein in hepatoma cell apoptosis and p53 expression. *Biotechnol Lett*. 2008;30:235–242.
17. Fox DK, Ebert SM, Bongers KS, Dyle MC, Bullard SA, Dierdorff JM, Kunkel SD, Adams CM. p53 and ATF4 mediate distinct and additive pathways to skeletal muscle atrophy during limb immobilization. *Am J Physiol Endocrinol Metab*. 2014;307:E245–E261.
18. Perry C, Kane DA, Lanza IR, Neuffer PD. Methods for assessing mitochondrial function in diabetes. *Diabetes*. 2013;62:1041–1053.
19. Coats AJ. Heart failure: what causes the symptoms of heart failure? *Heart*. 2001;86:574–578.
20. Hepple RT. Mitochondrial involvement and impact in aging skeletal muscle. *Front Aging Neurosci*. 2014;6:211.



# Supplemental Material

## Data S1.

### *Muscle biopsy*

Samples were taken from two sites in participants, including from the upper limb (pectoralis major) and lower limb (vastus lateralis). *Pectoralis major* sample was obtained during routine device implantation procedures, while on the same day a *vastus lateralis* sample of the right thigh were obtained using the Bergström needle method modified to allow for suction. The sample region was cleaned beforehand with iodine and anaesthetised (1% lidocaine), while the wound was closed with surgical tape strips and a soft adhesive sterile dressing. Biopsies were taken within 3 months following study recruitment and collection of baseline clinical data. There were no complications or adverse events with any of the research procedures. One piece of muscle sample was immediately placed in 1 mL of ice-cold specialized preservation solution termed BIOPS<sup>4</sup> for assessment of mitochondrial respiration while another small portion was rapidly frozen in a small subset for RNA sequencing.

### *Mitochondrial function*

Mitochondrial respiration was assessed *in situ* from saponin-permeabilized skeletal muscle fibres using high-resolution respirometry (Oxygraph-2K; Oroboros Instruments, Innsbruck, Austria), as previously described<sup>4</sup>. Briefly, in the following order: 1) complex I Leak respiration was determined by addition of glutamate (10 mM), malate (0.5 mM) and pyruvate (5 mM) (i.e., a measure of proton leak under non-phosphorylating conditions); 2) adenosine diphosphate (ADP; 2.5 mM) added to provide a measure of complex I oxidative phosphorylation (OXPHOS); 3) outer mitochondrial membrane integrity determined by addition of 10  $\mu$ M cytochrome c; 4) succinate at 10 mM as a complex II substrate provided complex I+II OXPHOS; 4) 5  $\mu$ M carbonyl cyanide 4-(trifluoromethoxy)-phenylhydrazone (FCCP) for maximal uncoupled complex I+II respiration; 5) complex I inhibitor rotenone at 0.25  $\mu$ M provided uncoupled complex II respiration; and 6) 2.5  $\mu$ M antimycin A as a complex III inhibitor for residual oxygen consumption (ROX) to calculate non-mitochondrial (background)

respiration, which was then used to normalise the data. Mitochondrial content was determined within the respirometer using a complex IV activity assay (a close proxy)<sup>4</sup> by the addition of 0.5 mM N,N,N',N'-Tetramethyl-p-phenylenediamine dihydrochloride (TMPD) as an artificial electron donor to complex IV in combination with 2 mM ascorbate to maintain TMPD in a reduced state. Absolute mitochondrial respiration was normalised to complex IV activity to provide an index of mitochondrial intrinsic function.

### *RNA isolation and sequencing*

In a subset of patients (CON = 3; CHF = 6) biopsies were immediately transferred to a clean 2 ml screw-capped tube and flash-frozen in liquid nitrogen. A small piece of tissue (~30 to 50 mg) was added to a 2 ml microcentrifuge tube containing a stainless-steel bead and 1 ml TRIzol (Invitrogen, UK). The tissue was homogenized using a TissueLyser (Qiagen, UK) at frequency 25 Hz for 2 minutes. RNA was extracted from the homogenate with TRIzol using standard protocols. Nine RNA samples were treated with DNase I using the RNA Clean and Concentrator kit (Zymo Research, UK). The quality of the RNA was evaluated on a DeNovix DS-11 FX + Spectrophotometer / Fluorometer (DeNovix, USA) as per manufacturer's instruction. RNA was considered of high quality when  $A_{260}/A_{280}$  and  $A_{260}/A_{230}$  ratios achieved 2.0. Subsequently, Agilent 2100 Bioanalyzer (Agilent Technology, USA) was used to measure RNA integrity number (RIN). Nine RNA samples achieved RIN value >7.5 and proceeded with RNA sequencing (RNA-seq). RNA-seq was performed using the TruSeq RNA library preparation kit at the Cambridge Genomics Services. The RNA-seq libraries were sequenced on the NextSeq 500 platform in a single lane, generating ~16 million single-end 75 bp reads for each sample (Table 4). All the protocols were carried out according to the manufacturer's recommendations. The raw reads were deposited at the ArrayExpress domain (<https://www.ebi.ac.uk/arrayexpress/>) under the accession E-MTAB-8531.

### *Bioinformatics processing*

Bioinformatics processing followed detailed methods published elsewhere.<sup>10</sup> Raw sequences in FASTQ format were downloaded from the sequencing centre. Quality control of the raw sequences were performed using *FastQC* v0.118 to evaluate the overall quality. The raw sequences were manipulated using *TrimGalore* v0.6.2 to remove the adapter sequences and low-quality sequences. Next, clean reads were mapped to the human reference genome (GRCh38 *Homo sapiens* reference genome release 96) using *STAR* v2.7 aligner. To improve the quality of the data, only uniquely mapping reads with a mapping quality score 255 were counted. Post-alignment quality control was carried out on all aligned BAM files. *featureCounts* v1.6.5 was used to quantify the read counts of each gene for the subsequently differential expression analysis. The expression profile of each gene was expressed as read counts.

#### *Differential expression analysis*

The raw read counts were used as an input for *DESeq2* v1.26, an R/Bioconductor package for differential expression analysis. *DESeq2* normalizes the raw read counts based on the median of ratios as described previously. Partial least squares discriminant analysis (PLS-DA), a supervised method implemented in *mixOmics* v6.10.2 was performed. PLS-DA was used to classify nine patients based on the *DESeq2* normalized counts for 18,426 genes. Two clusters in the PLS-DA plot consistently placed the nine samples into two groups. Recently, PLS-DA has been adapted to RNA-seq data to provide transcriptome expression landscape due to its ability to discriminate sample artefacts. Differentially expressed genes (DEGs) were conducted in a pairwise manner, using *DESeq2*. Genes achieving a false discovery rate (*FDR*) threshold below 0.05 were considered significantly differentially expressed. The full gene list is attached in Table S5. Volcano plot and heatmap of DEGs were constructed using the *ggplot2* package and '*pheatmap*' function implemented in *R*, respectively.



**Table S1. Demographic and clinical characteristics of cohort.**

	CHF (n=28)	CON (n=9)	P-value
<b>Demographics</b>			
Male sex [n (%)]	26 (93)	6 (67)	0.046
Age (years)	69.3±2.3	75.4±2.0	0.055
Weight (kg)	85.9±3.6	80.3±4.3	0.405
Height (m)	1.7±0.02	1.7±0.04	0.443
BMI (kg·m <sup>2</sup> )	29.5±0.9	26.9±1.3	0.156
<b>Clinical characteristics</b>			
NYHA class [n (%)]			
I	2 (7)	9 (100)	<0.001
II	16 (57)	0 (0)	
III	10 (36)	0 (0)	
IHD [n (%)]	16 (57)	2 (22)	0.068
DCM [n (%)]	10 (36)	0 (0)	0.036
AF [n (%)]	10 (36)	3 (33)	0.896
CABG [n (%)]	5 (18)	1 (11)	0.633
HTN [n (%)]	11 (39)	4 (44)	0.784
COPD [n (%)]	0 (0)	1 (11)	0.074
LVEF (%)	28.6±2.4	51.4±1.5	<0.001
LVIDd (mm)	49.9±2.4	31.4±2.4	<0.001
Hb (g·L <sup>-1</sup> )	141.7±3.0	129.9±6.6	0.073
Na (mmol·L <sup>-1</sup> )	139.7±0.6	140.6±0.9	0.490
K (mmol·L <sup>-1</sup> )	4.6±0.1	4.5±0.3	0.629
Creatinine (μmol·mL <sup>-1</sup> )	98.1±4.9	84.3±2.8	0.123
eGFR (mL·min <sup>-1</sup> ·1.73 m <sup>-2</sup> )	64.8±3.8	71.1±5.1	0.395
Glucose (mmol·L <sup>-1</sup> )	9.0±3.2	5.2±5.1	0.495
HbA1c (mmol·mol <sup>-1</sup> )	32.9±5.1	26.8±6.7	0.540

Data are mean±SEM and were assessed by unpaired Student's *t*-test. BMI, body mass index;  $\dot{V}O_{2peak}$ , peak pulmonary consumption; NYHA, New York Heart Association; IHD, ischaemic heart disease; DCM, dilated cardiomyopathy; AF, atrial fibrillation; CABG, coronary artery bypass graft; HTN, hypertension; COPD, chronic obstructive pulmonary disease; LVEF, left ventricular ejection fraction; LVIDs, left ventricular internal diameter in systole; LVIDd, left ventricular internal diameter in diastole; Hb, haemoglobin; Na, serum sodium; K, serum potassium; eGFR, estimated glomerular filtration rate; NT-pro-BNP, N-terminal pro hormone B-type natriuretic peptide; HbA1c, glycated haemoglobin.

**Table S2. Medications and device therapy.**

	CHF (n=28)	CON (n=9)	P-value
<b>Medications</b>			
ACEi [n (%)]	22 (79)	2 (22)	0.002
Beta-blocker [n (%)]	27 (96)	1 (11)	<0.001
Furosemide equivalent dose (mg)	33.6 ± 6.4	8.9 ± 8.9	0.055
ARB [n (%)]	5 (18)	1 (11)	0.633
MRA [n (%)]	13 (46)	1 (11)	0.057
Statin [n (%)]	20 (71)	6 (67)	0.786
Antiplatelet [n (%)]	14 (50)	1 (11)	0.039
Metformin [n (%)]	6 (75)	0 (0)	0.129
Insulin [n (%)]	2 (7)	0 (0)	0.410
Sulphonylurea [n (%)]	3 (11)	0 (0)	0.306
Anticoagulant [n (%)]	7 (25)	5 (56)	0.218
Digoxin [n (%)]	4 (14)	0 (0)	0.230
Ivabradine [n (%)]	1 (4)	0 (0)	0.565
<b>Device therapy</b>			
PPM [n (%)]	0 (0)	9 (100)	<0.001
ICD [n (%)]	6 (21)	0 (0)	0.129
CRT [n (%)]	22 (79)	0 (0)	<0.001

Continuous variables are presented as mean±SEM, categorical variables as number (%) and were assessed by unpaired Student's t-test. ACEi, angiotensin-converting enzyme inhibitor; ARB, angiotensin receptor blocker; MRA, mineralocorticoid receptor antagonist; PPM, permanent pacemaker; ICD, implantable cardioverter defibrillator; CRT, cardiac resynchronisation therapy.

**Table S3. Demographic and clinical characteristics for participants included in the RNAseq analysis.**

	CHF (n=6)	CON (n=3)	P-value
<b>Demographics</b>			
Male sex [n (%)]	6 (100)	2 (67)	0.13
Age (years)	76.7 ± 3.3	80.2 ± 2.6	0.51
Weight (kg)	77.2 ± 7.5	74.5 ± 20.7	0.85
Height (m)	1.7 ± 0.05	1.7 ± 0.1	0.62
BMI (kg·m <sup>2</sup> )	27.6 ± 1.7	24.9 ± 1.9	0.37
<b>Clinical characteristics</b>			
NYHA class			
I	2 (33)	3 (100)	0.17
II	2 (33)	0 (0)	
III	2 (33)	0 (0)	
IHD [n (%)]	3 (50)	1 (33)	0.64
DCM [n (%)]	3 (50)	0 (0)	0.13
AF [n (%)]	3 (50)	1 (33)	0.64
CABG [n (%)]	2 (33)	1 (33)	1.0
HTN [n (%)]	3 (50)	3 (100)	0.13
COPD [n (%)]	0 (0)	1 (33)	0.13
LVEF (%)	26.3 ± 5.6	50.8 ± 3.0	0.006
LVIDd (mm)	56.5 ± 3.6	49.7 ± 2.4	0.26
Hb (g·L <sup>-1</sup> )	143.0 ± 3.7	114 ± 13.9	0.029
Na (mmol·L <sup>-1</sup> )	143.0 ± 1.0	138.7 ± 1.2	0.039
K (mmol·L <sup>-1</sup> )	4.3 ± 0.2	4.4 ± 0.7	0.88
Creatinine (μmol·mL <sup>-1</sup> )	96.7 ± 8.5	86.0 ± 7.0	0.45
eGFR (mL·min <sup>-1</sup> ·1.73 m <sup>-2</sup> )	67.7 ± 6.9	69.0 ± 12.1	0.92
HbA1c (mmol·mol <sup>-1</sup> )	39.4 ± 1.2	44.0	-

Continuous variables are presented as mean ± SEM, categorical variables as number (%). BMI, body mass index;  $\dot{V}O_{2peak}$ , peak pulmonary consumption; NYHA, New York Heart Association; IHD, ischaemic heart disease; DCM, dilated cardiomyopathy; AF, atrial fibrillation; CABG, coronary artery bypass graft; HTN, hypertension; COPD, chronic obstructive pulmonary disease; LVEF, left ventricular ejection fraction; LVIDs, left ventricular internal diameter in systole; LVIDd, left ventricular internal diameter in diastole; Hb, haemoglobin; Na, serum sodium; K, serum potassium; eGFR, estimated glomerular filtration rate; NT-pro-BNP, N-terminal pro hormone B-type natriuretic peptide; HbA1c, glycated haemoglobin.

**Table S4. Summary statistics of RNA sequencing, total number of reads generated, read mapping to the GRCh38 *Homo sapiens* reference genome, RNA integrity number (RIN), for nine RNA samples.**

<b>Sample</b>	<b>Raw reads</b>	<b>Unique reads</b>	<b>Percentage of mapped reads</b>	<b>RIN score</b>
<b>SKM_C_1</b>	16216274	15022715	92.64	8
<b>SKM_C_2</b>	18364747	16835780	91.67	7.5
<b>SKM_C_3</b>	20400222	18670124	91.52	8.2
<b>SKM_HF_1</b>	14233566	13140795	92.32	8.6
<b>SKM_HF_2</b>	16437260	15135973	92.08	8.8
<b>SKM_HF_3</b>	14932640	13646610	91.39	7.6
<b>SKM_HF_4</b>	15333154	14116260	92.06	8.5
<b>SKM_HF_5</b>	14537174	13352387	91.85	8.9
<b>SKM_HF_6</b>	15308095	14092935	92.06	7.9



**Table S5. Gene database.** Please see Excel file.

**Table S6. Demographic and clinical characteristics from two apparently distinct clusters of patients with CHF derived from the RNAseq analysis.**

	Cluster 1 (1,3,4)	Cluster 2 (2,5,6)	P-value
<b>Demographics</b>			
Male sex [n (%)]	3 (100)	3 (100)	1.0
Age (years)	76.1 ± 12.6	77.2 ± 0.8	0.88
Weight (kg)	80.7 ± 7.2	73.7 ± 27.6	0.69
Height (m)	1.7 ± 0.1	1.6 ± 0.2	0.68
BMI (kg·m <sup>2</sup> )	28.3 ± 2.9	26.8 ± 5.8	0.70
<b>Clinical characteristics</b>			
NYHA class [n (%)]			
I	0 (0)	2 (67)	0.14
II	1 (33)	1 (33)	
III	2 (67)	0 (0)	
IHD [n (%)]	2 (67)	1 (33)	0.41
DCM [n (%)]	1 (33)	2 (67)	0.41
AF [n (%)]	1 (33)	2 (67)	0.41
CABG [n (%)]	1 (33)	1 (33)	1.0
HTN [n (%)]	2 (67)	1 (33)	0.41
COPD [n (%)]	0 (0)	0 (0)	.
LVEF (%)	38.3 ± 5.8	14.2 ± 1.4	0.002
LVIDd (mm)	52.0 ± 7.8	61.0 ± 8.7	0.25
Hb (g·L <sup>-1</sup> )	138.7 ± 4.0	147.3 ± 11.5	0.29
Na (mmol·L <sup>-1</sup> )	144.3 ± 2.5	141.7 ± 2.1	0.23
K (mmol·L <sup>-1</sup> )	4.2 ± 0.5	4.3 ± 0.6	0.84
Creatinine (μmol·mL <sup>-1</sup> )	85.7 ± 22.1	107.7 ± 15.5	0.23
eGFR (mL·min <sup>-1</sup> ·1.73 m <sup>-2</sup> )	76.7 ± 19.1	58.7 ± 10.8	0.23
HbA1c (mmol·mol <sup>-1</sup> )	40.0 ± 3.6	38.5 ± 2.1	0.64

Data are mean±SEM and were assessed by unpaired Student's *t*-test. BMI, body mass index;  $\dot{V}O_{2peak}$ , peak pulmonary consumption; NYHA, New York Heart Association; IHD, ischaemic heart disease; DCM, dilated cardiomyopathy; AF, atrial fibrillation; CABG, coronary artery bypass graft; HTN, hypertension; COPD, chronic obstructive pulmonary disease; LVEF, left ventricular ejection fraction; LVIDs, left ventricular internal diameter in systole; LVIDd, left ventricular internal diameter in diastole; Hb, haemoglobin; Na, serum sodium; K, serum potassium; eGFR, estimated glomerular filtration rate; NT-pro-BNP, N-terminal pro hormone B-type natriuretic peptide; HbA1c, glycated haemoglobin.